Asset Integrity Monitoring of Wind Turbine Blades with Non-Destructive Radar Sensing

Jamie Blanche
Smart Systems Group, Institute of Sensors, Signals and Systems
Heriot-Watt University
Edinburgh
United Kindom
j.blanche@hw.ac.uk

Daniel Mitchell
Smart Systems Group, Institute of Sensors, Signals and Systems
Heriot-Watt University
Edinburgh
United Kindom
daniel.mitchell@hw.ac.uk

Ranjeetkumar Gupta
Smart Systems Group, Institute of Sensors, Signals and Systems
Heriot-Watt University
Edinburgh
United Kindom
r.gupta@hw.ac.uk

Adrian Tang
Smart Systems Group, Institute of Sensors, Signals and Systems
Heriot-Watt University
Edinburgh
United Kindom
at23@hw.ac.uk

David Flynn
Smart Systems Group, Institute of Sensors, Signals and Systems
Heriot-Watt University
Edinburgh
United Kindom
d.flynn@hw.ac.uk

***Abstract*— Global growth in onshore and offshore wind energy has created a forecasted 11.5% Compound Annual Growth Rate (CAGR) increase in Wind Turbine (WT) blades throughout 2020-2025. The ability to verify blade condition throughout the asset lifecycle is integral to economic and reliable renewable energy supplies. Currently, commercial inspection of deployed wind turbine blades is predominately performed by rope access personnel using visual and infrared cameras. In this paper we present the results of Frequency Modulated Continuous Wave (FMCW) radar analysis of a decommissioned wind turbine blade exhibiting clearly defined defects. We show that FMCW sensing provides a non-invasive, non-destructive and non-contact means of surface and sub-surface integrity evaluation of these composite structures. We observe absolute unit (a.u.) order of magnitude contrasts for healthy blades at 0.47 x10^6 (a.u.) versus defective blade structures at 1.9 x10^5 (a.u.). Our results present the analysis of the decoupled reflected electromagnetic wave, verifying FMCW sensitivity to different failure modes relating to surface and internal structures of the WT blade. The FMCW analysis of WT blades demonstrated within this paper represents a first in instantaneous cross-sectional analysis of blade assets, providing a transformative advancement in WT blade integrity analysis.**

Keywords*— *Asset Integrity Inspection, Frequency Modulated Continuous Wave Radar, Microwave Sensing, Non-Destructive Testing, Offshore Renewable Maintenance, Wind Turbines

I. INTRODUCTION

The complex multi-objective optimization of energy security, energy equity and environmental sustainability represents a global energy trilemma, where the demand and requirement for decarbonization represents a world-wide issue for nations and commercial sectors committed to addressing unsustainable greenhouse gas emissions. Sustainable wind energy farms have played a vital role in maintaining a carbon emission balance, however a major hindrance to offshore renewable wind sector advancement is the extensive utilization of composite structures. Composite materials have been proven to improve cost-effectiveness but also pose a significant challenge in structural integrity assessment, damage interpretation and repair strategies. Composite structures rarely exhibit early signs of damage progression, when compared to metal component equivalents which undergo well-defined corrosion pathways. The lack of such observable damage progression in major wind turbine asset components incurs significant monitoring costs with severe damage consequences [1].

The COVID-19 crisis has driven the largest human-driven carbon crash ever recorded. Energy demand within the UK reduced by approximately 75% during the UK-wide lockdown and the National Grid responded by removing high emission power plants from the network. This reduction in energy demand resulted in a national two-month cessation in coal fired power generation [2–5]. This transfer of supply was possible solely due to extensive renewable energy investment in the UK. Governments were encouraged to maximize the opportunity to achieve carbon emissions reduction targets by investing in more renewable energy infrastructure. The Global Wind Energy Council advises that wind power will play a key role as a building block for global economic recovery from the impact of COVID-19 [6]. In 2019, the UK successfully reduced carbon emissions whilst growing the economy by

Funded by Engineering Physical Sciences Research Council (EPSRC) Offshore Robotics for the Certification of Assets (ORCA) Hub [EP/R026173/1] and EPSRC Holistic Operation and Maintenance for Energy from Offshore Wind Farms (HOME) [EP/P009743/1] projects.

978-1-7281-8416-6/20/$31.00 ©2020 IEEE

72%, however, meeting new climate targets will require new strategies [7].

Prior to the COVID-19 crisis, significant expansion of global offshore energy by ~17% annual growth was predicted, from 22 GW to 154 GW in total installed capacity by 2030, with the UK potentially contributing up to 30GW of this generating capacity [8]. Scotland has established the capability to produce large wind farms with the recent commissioning of eighty-four, 7MW wind turbines at the Beatrice Offshore Wind Farm, approximately 13 km off the Caithness coast [9–11]. Presently, the development of such wind farms does not confirm that these targets will be realized as projected, as only uninterrupted service delivered by each of the individual wind turbines within the wind farm can guarantee this level of target attainment. This drive for optimal performance reinforces the importance of a robust and active Structural Health Monitoring (SHM) system, where SHM represents a means of regular asset integrity monitoring and often utilizes deployed or embedded sensing to detect departures from a baseline measurement representative of the healthy structure. The development and application of composite materials in the offshore energy sector has enabled new designs and gains in blade performance while also presenting new and distinct challenges to both deployable and embedded SHM sensing modalities. Fig. 1 summarizes various methods of Non-Destructive Techniques (NDT); that are used for composite damage detection or SHM, and highlights their associated limitations [12–14].

Based on this summary and previous studies [15–21], it is understood that Frequency Modulated Continuous Wave (FMCW) radar sensing is a high potential candidate technology that is uniquely suited to detailed non-contact and non-destructive analysis of composite structures. The millimetre-wave sensing modality exhibits minimal limitations when compared to currently employed methods for external and internal asset inspection. The major advantage of FMCW in the K-band is the ability to penetrate low dielectric materials and return data for amplitude extractions via Fourier transforms and other data analytical techniques. FMCW is also resilient to harsh environments with low power draw and non-harmful radiation. The ability to monitor a Wind Turbine (WT) blade asset from a practical non-contact and non-invasive range (~2 - 10 metres) in dynamic conditions, with a tunable sensor to inspect surface and sub-surface internal structures, is highly desirable for offshore WT blade inspections. In this paper we investigate a decommissioned blade and perform experimental analysis of the FMCW radar for key, internal failure modes and failure precursors. This research represents a lab-based, simulated scenario where a drone-mounted or handheld sensor has been deployed to inspect an offshore asset for blade SHM aimed at the prevention of further operationally induced deterioration, thus increasing the effectiveness of vital carbon reduction infrastructure.

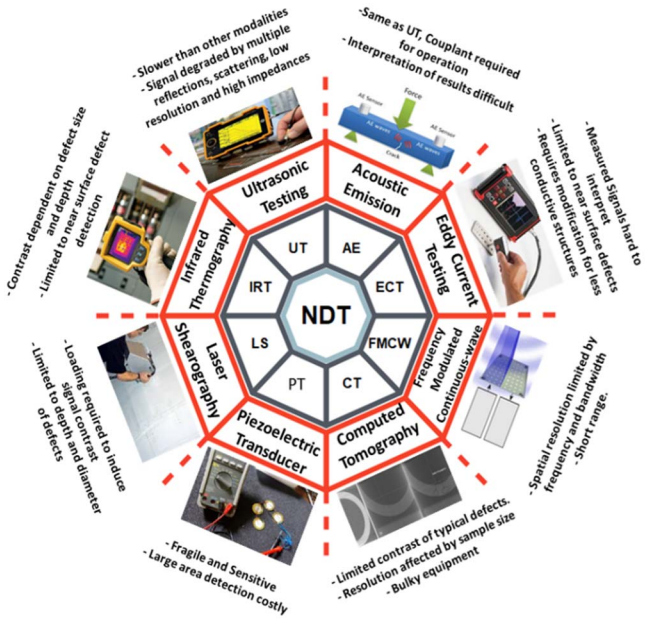

Fig. 1 Graphical summary of various existing methods of composites NDT with their major associated limitations

TABLE 1 DESCRIPTION OF FAILURE MODES ON WIND TURBINE BLADES [23]

Type	Description
1	Adhesive layer damage formation and growth in bond joining skin and main spar flanges (skin/adhesive debonding)
2	Adhesive layer damage formation joining the up- and downside skins along leading and trailing edges (adhesive joint failure)
3	Damage formation and growth at the interface between face and core in sandwich panels in skins and main spar web
4	Internal damage formation and growth in laminates in skin and/or main spar flanges, under tensile or compression load
5	Laminate skin and main spar splitting and fracture of separate fibers (fiber failure in tension; laminate failure in compression)
6	Buckling of skin due to damage formation and growth in the skin and main spar bond under compressive load (skin/adhesive debonding induced by buckling, a specific type 1 case)
7	Formation and growth of cracks in the gel-coat; debonding of the gel-coat from the skin (gel-coat cracking and gel-coat/skin debonding)

The remainder of this paper is structured as follows; Section II introduces the decommissioned wind turbine blade utilized as our test specimen. A full description of typical failure modes is also provided. Section III describes the theory of FMCW sensing. Section III.A characterizes the antenna and Section III.B outlines the sensor parameters and data acquisition workflow. The experimental procedure and methodology are presented in Section IV. Preliminary results from the microwave analysis of the blade are presented in Section V. Section VI discusses the acquired results and presents recommendations for further analysis of WT blades with FMCW technology. Section VII concludes.

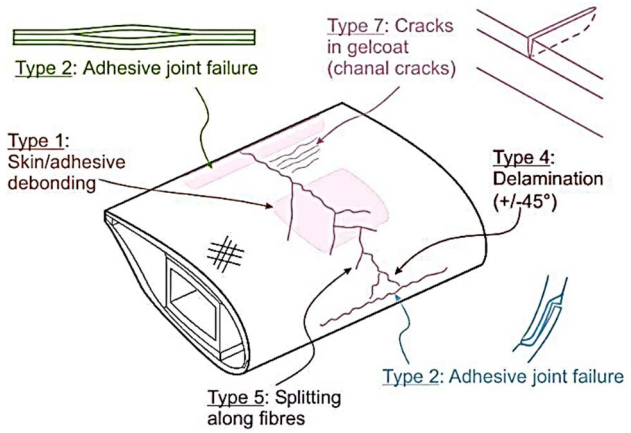

Fig. 2 Schematic of common modes of wind turbine blade failures [24]

Fig. 3 Sample of defective wind turbine blade showing type 4 delamination detail and area used for the ingress of water during testing. K-band FMCW antenna visible 10 cm to right of structure. Note: delamination situated at internal blade structure and not visible from blade exterior

II. Decomissioned Wind Turbine Blade and Failure Modes

Wind turbine blades are constructed using a range of composites, epoxy resins and adhesives. The structure is exposed to significant static and dynamic lift forces, gravitational loads and aerodynamic drag over their expected 20-year life cycle [22]. The strengthening of WT blades, via use of composite materials, is well documented with refinements in offshore WT designs aimed at decreasing the cost of manufacturing, whilst increasing the operational lifespan of these high-value offshore assets [1]. WT blades are susceptible to several distinct types of failures which are categorized from type 1 – 7 [23]. These failure types distinguish the type of fault and location and are fully described in Table 1, with common faults illustrated in Fig. 2. Delamination features observed within our blade specimen (Fig. 3) are the key target for this series of experiments, with a contrast in Return Signal Amplitude (RSA) expected for areas of increased porosity within the sample, versus those acquired for undamaged baseline areas. The chosen type of defect, a type 4 delamination, is situated on the inside surface of the composite wind turbine blade structure and would not be visible from the asset exterior under normal operating conditions. Detection of this type of hidden, sub-surface defect represents a key and critical challenge to current asset integrity inspection modes, where the identification of such features typically requires contact or invasion of the asset structure.

A commonly occurring defect in wind turbine blades, via operationally induced stresses or manufacturing defects, is the formation of delaminated areas of the airfoil composite structure, which provokes an increase in inter-laminar shear stress. Cracking or distortions, due to impacts during installation or loads exceeding acceptable yield stress may be identified as both longitudinal and transverse cracks, with an observed, highly-localized increase in material porosity. Frozen moisture is a form of defect arising from a combination of porosity and moisture penetration into gaps following leading-edge erosion. This ingress of moisture freezes in the sub-zero temperatures induced by cold air flow across the moving blade. The specific weaving pattern of fiber-reinforced plastic can induce defects such as fiber wrinkling, gaps, misalignment or waviness, classified as deformation. FMCW in the K-band is particularly sensitive to porosity and the experimental work presented in this paper will address these specific defects and their key measurands for microwave sensing.

III. Radar and Dielectric Theory

The relative permittivity, ε_r^* of material components, defined as the dielectric relaxation processes for each composite material, govern Electro-Magnetic (EM) wave attenuation and dispersion. These relaxation processes, influenced by the frequency of incident radiation, damp induced localized oscillations at differing rates as a function of component scale range. Key feature extractions inform material properties and are derived from data returned to the sensor by the reflected radar signal. The observed RSA is affected by many factors in low-dielectric porous materials. These include interfacial geometry, surface contaminants, fluid content and type and the abundance of high permittivity minerals.

FMCW represents a continuous frequency swept output and differs from higher power, pulsed-wave radars. Modulation of the continuous wave provides a frequency change over time to create a saw-tooth (or triangular) frequency output, as illustrated in Fig. 4. The difference between the transmitted and received signal frequencies is determined by the convolution of the input and output waves to give a new, lower intermediate frequency (IF) signal. The IF is then analysed to calculate the distance and velocity parameters of an object within the sensor field of view. This IF signal is transmitted to a data logger as a signal of frequency Δf. An overview of the determination of the IF signal is as follows:

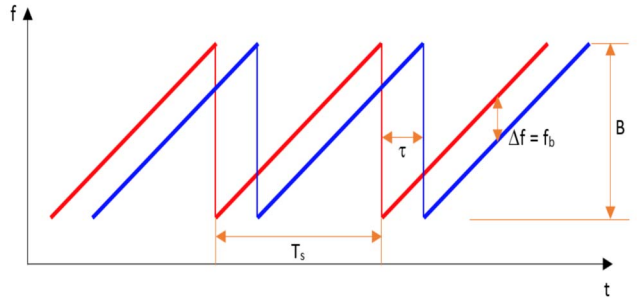

Fig. 4 "Sawtooth" mode of transmitted and received signals from the radar module, where f = frequency, t = time, Ts = sweep duration, τ = two way travel time of return signal, B = sweep bandwidth and Δf = intermediate frequency [21]

$$f_{RF_{out}} = f_{RF_0} + k_f \times t \tag{1}$$

where $0 \leq t \leq T_s$, f_{RF_0} is the initial frequency, T_s is the frequency sweep time (chirp duration) and k_f is the sweep rate.

$$k_f = \frac{B}{T_s} \tag{2}$$

where, B is the frequency sweep bandwidth, the round trip, two-way time, where $\Delta t = \tau$, of the emitted signal is calculated as:

$$\tau = 2\frac{d}{c} \tag{3}$$

where d is the distance between the reflecting target and antenna and c is the speed of light in the medium of propagation.

In all cases, we are assuming the speed of light in air to be equal to the speed of light in a vacuum. Therefore, due to the observed delay in return signal, the return frequency compared to the emitted frequency will be:

$$f_{RFreceived} = f_{RF0} + k_f * (t - \tau) \tag{4}$$

where, $\tau \leq t \leq T_s + \tau$. The intermediate frequency (Δf) between the emitted and received signal is therefore:

$$\Delta f = k_f * (-\tau) \tag{5}$$

The following expression can be used if the negative time of flight is taken as a magnitude:

$$\Delta f = \frac{B}{T_s} * 2\frac{d}{c} \tag{6}$$

Due to the relationship expressed in (6), the distance between the sensor and the target is kept constant to extrapolate key amplitudinal measurands pertaining to the target properties. Thereby, any amplitudinal signal variation detected for a specific distance from the antenna can be clearly attributed to the intrinsic properties of the target and asset condition contrasts, such as fluid influx or delamination. However, where the target distance cannot be maintained easily, the application of a library of known "ideal target reflector" responses for the full range of distances from the sensor for a specific target can be applied to compare with the acquired signal contrasts. Full descriptions of FMCW radar interaction between porous media partially saturated with fluids and internal properties via non-invasive FMCW measurement are provided in Blanche (2018) [18] and Blanche (2020) [19]. The remainder of this section will present the characterization of sensing equipment and data acquisition methods used for this research.

A. Antenna Characterization

To obtain a profile of the radiative output of a Flann K-band antenna model: #21240-20/serial: #219405, a vector network analyser (VNA) output was configured to emit a K-band, frequency-swept signal, while connected to the antenna via a high-frequency Pasternack coaxial waveguide. A two-dimensional translation stage was used to perform three scans coupled to a WR42 type OEWG (open-ended waveguide) standard probe for the K-band (18-26.5 GHz), and using a non-radiative near-field separation distance between the probe and the antenna of 100 mm. Data sets were acquired to represent the 1500 MHz bandwidth sweep used in the radar module. Fig. 5A shows the 2D radiation pattern acquired. Fig. 5B illustrates the phase shift characteristic of the same antenna - VNA configuration.

The purpose of this characterization work was to quantify the sample area on the target. This was determined as being within a consistent radius, if all work was conducted at a fixed sample - antenna distance of 100 mm. The Flann microwave antenna was shown to display a radiation pattern dispersal characteristic with a peak amplitude representing a spot size on the target of ~36.4 mm radius at a separation of 100 mm with a minimal phase differential and representing the effective field of view of the sensor.

B. Frequency Modulated Continuous Wave Equipment Parameters and Data Acquisition Workflow

Fig. 6 shows a block diagram of the experimental setup and procedure, which can be divided into 6 main stages [18-21]:

a) Signal generator creating a sawtooth wave with a 1.5 GHz (24 – 25.5 GHz) bandwidth and with a 300-millisecond chirp duration. Data acquisition rate was once per second (Table 2),

b) Flann Microwave model #21240-20 (rated 17.6 - 26.7 GHz) standard gain horn antenna (serial #219405) with a nominal gain of 20 dBi at 22.15 GHz. This antenna was attached to a static mounting directed squarely onto the wind turbine section and at a constant distance of 100 mm,

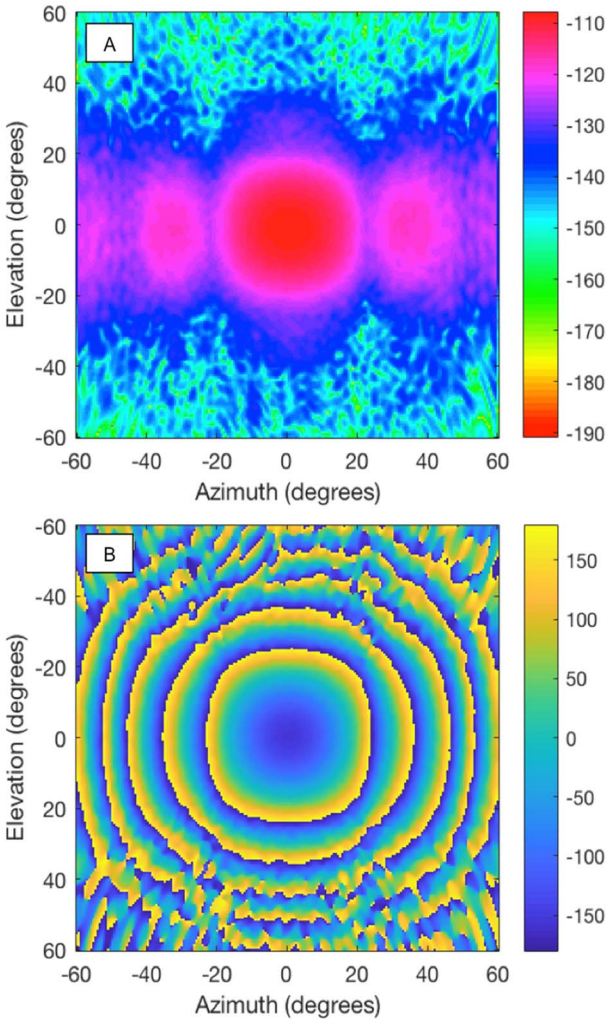

Fig. 5 A) 2D K-Band radiation pattern for amplitude for Flann Microwave antenna model #21240-20 (scale bar in dBm). B) 2D K-Band radiation pattern for phase shift for Flann Microwave antenna model #21240-20 (scale bar in degrees) [21]

c) FMCW inspection target. In this asset SHM use case, a wind turbine section with observed type 4 defect was used (Table 1),

d) MATLAB 2018a was used to create a Graphical User Interface (GUI), which acquired data for analytical processing,

e) Reference and return signal waveforms were convolved to generate an intermediate frequency (IF), as shown in (6),

f) Data processing was performed via Fourier transform into the frequency domain, from which amplitude extractions were analysed and presented. Data analysis time is 31 milliseconds and datasets are stored to build a library of material responses for the detection of contrast agents.

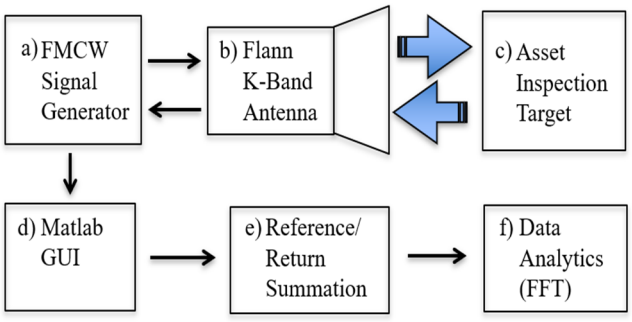

Fig. 6 Block diagram of analytical procedure and experimental setup showing hardware components and basic data processing steps [21]

TABLE 2 FMCW PARAMETERS USED DURING WIND TURBINE DEFECT TRIALS

Parameter	**Value**
Band	K – Band (24 – 25.5 GHz)
Chirp Duration	300 milliseconds
Bandwidth	1500 MHz
Acquistion Frequency	1 Hz (0.2 – 3 Hz tunable)

IV. EXPERIMENTAL SETUP AND METHODOLOGY

These experiments were designed to test the effect of water ingress and the sensitivity of the K-band FMCW radar to contrasts resulting from the addition of water within the sensor field of view [25]. The standard separation of 100 mm was employed, resulting in a field of view on the target of 4.2 $x10^{-3}$ m^2.

The antenna was positioned so that the direction of EM propagation was perpendicular to the blade interface as shown in Fig. 3. For experiment A, a healthy section of the blade was scanned to establish a baseline measurement. The radar was then positioned adjacent to a section of delaminated blade structure. For experiment B, the procedure for experiment A was repeated, where FMCW data was continuously acquired for the delaminated area. A contrast agent of 3 ml of water was deposited within the delamination defect and within the field of view of the sensor. The results from these tests are shown in Section V.

V. DATA ANALYSIS AND RESULTS

A. Contrast Between Baseline and Delamination Test

This section presents baseline tests to assess the sensitivity of K-band FMCW to contrasts in wind turbine blade structure integrity. Fig. 7 shows the difference in RSA for a wooden core section of wind turbine blade with no defects and a section of wooden core of similar parameters of composite structure and thickness but exhibiting type 4 defect damage, as fully described in Table 1 and shown in Fig. 3. The healthy baseline measurement shows a peak at bin 5, corresponding to a distance from the sensor of 100 mm, of RSA 0.47 $x10^6$ (a.u.),

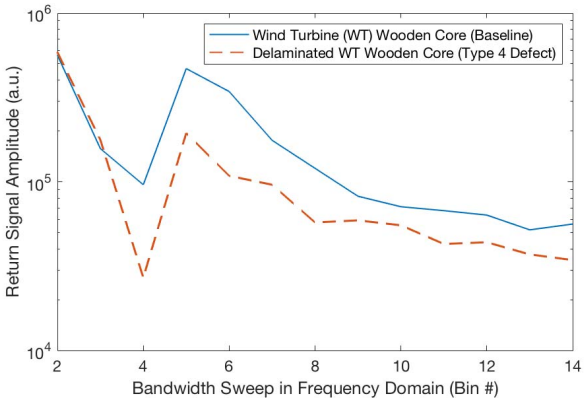

Fig. 7 Comparison of return signal amplitudes in the frequency domain for a healthy section of wind turbine blade wooden core structure versus a section of wooden core exhibiting a type 4 defect (see Table 1 and Fig. 3)

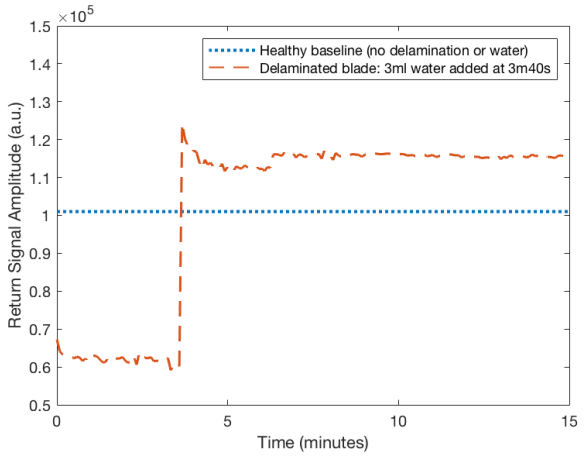

Fig. 8 Dynamic return signal amplitude of water ingress to an area of internal delamination within a wind turbine blade structure. Water added to type 4 defect at 3 mins and 40 seconds into experiment

with a type 4 defect giving an RSA of 1.94 x10^5 (a.u.). This significant contrast in RSA validates the use of K-band FMCW to discriminate between healthy and defective sections of wind turbine core structures. This contrast is visible at both the primary interface at bin 5 and in the delayed returns between bin 5 and bin 14+. These delayed returns give valuable data regarding the pore contents in porous composite materials and represent the many interfaces present within a porous composite structure. Section VB will present results acquired for small volume fluid ingress within the same delamination feature.

B. Water Ingress within Delamination Defect

The results for water ingress within a type 4 delaminated wind turbine blade structure are illustrated within Fig. 8. For this test, the data shown represent dynamic conditions at bin 7, an area beyond the first interface observed at bin 5 in Fig. 7 and thus representative of a bulk volume of the internal structure of the wind turbine composite laminate skin structure. From this data, the following is observed:

- The RSA of a healthy baseline (undamaged) area of the turbine blade structure is approximately 1.0×10^5 (a.u.) (i.e. low dielectric of constant thickness and as expected for a structure made of porous polymers reinforced by layered carbon fiber and glass resins).
- The RSA of the damaged, delaminated area of turbine blade structure ranges between 0.65 and 0.7×10^5 (a.u.) (i.e. lower dielectric than the healthy baseline value due to increased porosity and inconsistent thickness).
- The addition of 3 ml of water into the delamination at 3 minutes and 40 seconds, while obscured from the sensor by ~2 cm of porous polymer and retained by the inner carbon fiber/glass resin layer, results in a clear and immediate contrast in RSA that is significant and distinct from the healthy baseline.

VI. Discussion

This research presents a novel application of FMCW radar sensing to surface and subsurface structural analysis of a decommissioned wind turbine blade to identify distinct defects and their key measurands. The findings reported here have established that sensing of composite materials provides significant contrast in the RSA, allowing for detection of delamination and water ingress in the interior structure of a wind turbine blade. This work highlights the suitability of FMCW radar to act as a discriminator for the presence of porosity features within a vulnerable and compromised asset structure and to identify both frozen and liquid phases within a turbine blade structure. This will prevent further deterioration of a turbine blade structure, increasing the operational effectiveness of a vital carbon reduction asset. FMCW radar sensing represents an advancement of NDT methods for the real-time detection of faults. The advantages offered to SHM practices for the renewables sector include non-contact and non-destructive methods that are unaffected by mist, fog and smoke. The versatility of K-band FMCW sensing will improve the current state-of-the-art in defect detection strategies, such as visual and thermal inspection, which can be augmented in future operations with integration to FMCW systems, coupled with advanced digital analysis and digital twin systems. By providing real-time, front end asset integrity analytics, a FMCW augmented sensor suite will enable accurate monitoring of faults, defects, planning of maintenance and remaining useful life of asset datasets for integration within digital twin systems for intelligent asset field control.

VII. Conclusion

This paper highlights the increase in demand for NDT sensing to evaluate the state of a wind turbine blade. A literature review has been conducted to evaluate the effectiveness of the state-of-the-art in NDT and discusses the relative advantages of FMCW sensing within this sector. A decommissioned wind turbine blade was utilized to evaluate the effectiveness of the sensor for surface and subsurface faults within the composite. These experiments included

investigation of the return signal amplitude for an area classified as undamaged and compared to a delaminated section of wind turbine blade. The sensor then evaluated the effect of 3 ml water ingress when applied to a type 4 internal structure delamination defect.

Further work to improve experimental strategies for material and defect type characterization will include:

- High frequency sensing in the THz band, where the acquisition of higher resolution data is offset by a reduction in sensor range.
- The incorporation of dielectric lensing to reduce radiation pattern divergence will allow for the minimization of peak amplitude spot size on the target while allowing for a greater stand-off distance from the asset for the same power output.
- Tunable dielectric lensing will enable an operator to focus on a specific area of the turbine blade or to perform a wider sweep of an asset.
- Increasing the practical range to target will be a key step in the operational deployment of the FMCW sensor in the harsh offshore operating environment, facilitating integration with robotically deployed sensor suites capable of longer distance asset inspection and routine observations and capitalizing on the platform agnostic potential of the sensor.

As wind turbine technology continues to advance, offshore wind farm sites favor the installation of larger wind turbines, in larger arrays, in deeper water and situated further offshore. Integration of the FMCW sensor suite with trusted autonomous robotic systems will allow improvements in asset management efficiency, saving costs in OPEX and CAPEX while preserving the longevity of the renewable energy asset in the far offshore environment.

ACKNOWLEDGMENT

This research has been supported by MicroSense Technologies Ltd (MTL) in the provision of their patented microwave sensing technology (PCT/GB2017/053275) and wind turbine blade section.

REFERENCES

[1] R. Gupta, D. Huo, M. White, V. Jha, G. B. G. Stenning, and K. Pancholi, “Novel method of healing the fibre reinforced thermoplastic composite: A potential model for offshore applications,” *Compos. Commun.*, vol. 16, pp. 67–78, 2019, doi: 10.1016/j.coco.2019.08.014.

[2] “Britain goes coal free as renewables edge out fossil fuels - BBC News.” [Online]. Available: https://www.bbc.co.uk/news/science-environment-52973089. [Accessed: 14-Jun-2020].

[3] “Five key questions about energy after Covid-19 - BBC News.” [Online]. Available: https://www.bbc.co.uk/news/science-environment-52943037. [Accessed: 14-Jun-2020].

[4] “Drax Electric Insights.” [Online]. Available: https://electricinsights.co.uk/#/dashboard?period=3-months&start=2020-03-12&&_k=ookxqg. [Accessed: 14-Jun-2020].

[5] I. Staffell, R. Green, R. Gross, T. Green, L. Clark, and Drax, “Quarterly-Electricity Insights-January to March 2020,” 2020.

[6] Global Wind Energy Council, “Wind Power a cornerstone of the Global Economic Recovery,” Brussels.

[7] BiGGAR Economics, “Beatrice Building for the future Socio-economic benefits and learnings,” 2019.

[8] “Offshore wind Sector Deal - GOV.UK.” [Online]. Available: https://www.gov.uk/government/publications/offshore-wind-sector-deal/offshore-wind-sector-deal#fn:1. [Accessed: 14-Jun-2020].

[9] “Home | beatricewind.” [Online]. Available: https://www.beatricewind.com [Accessed: 14-Feb-2020].

[10] A. Hendry, “£2.5bn Beatrice offshore wind farm officially opened in Wick by Duke of Rothesay,” 2019. [Online]. Available: https://www.johnogroat-journal.co.uk/news/2-5bn-beatrice-offshore-wind-farm-officially-opened-in-wick-by-duke-of-rothesay-180982/. [Accessed: 19-Feb-2020].

[11] “Beatrice Exhibition Board Nov 2014.” [Online]. Available: https://sse.com/media/277452/BeatriceExhibitionBoardsNov14.pdf. [Accessed: 20-Feb-2020].

[12] C. Tushar *et al.*, “8 - Maintenance and monitoring of composites,” in *Woodhead Publishing Series in Composites Science and Engineering*, M. Jawaid, M. Thariq, and N. B. T.-S. H. M. of B. Saba Fibre-Reinforced Composites and Hybrid Composites, Eds. Woodhead Publishing, 2019, pp. 129–151.

[13] X. Qing, W. Li, Y. Wang, and H. Sun, “Piezoelectric Transducer-Based Structural Health Monitoring for Aircraft Applications,” *Sensors (Basel).*, vol. 19, no. 3, p. 545, Jan. 2019, doi: 10.3390/s19030545.

[14] H. Towsfyan, A. Biguri, R. Boardman, and T. Blumensath, “Successes and challenges in non-destructive testing of aircraft composite structures,” *Chinese J. Aeronaut.*, vol. 33, no. 3, pp. 771–791, 2020, doi: https://doi.org/10.1016/j.cja.2019.09.017.

[15] J. Blanche, D. Flynn, H. Lewis, G. D. Couples, and R. Cheung, “Analysis of geomaterials using frequency modulated continuous waves ,” *13th International Conference on Condition Monitoring and Machinery Failure Prevention Technologies 2016* . 10-Oct-2016.

[16] J. Blanche, D. Flynn, H. Lewis, G. Couples, and R. Cheung, “Analysis of Geomaterials using Frequency Modulated Continuous Wave Radar in the X-band,” *IEEE 26th Int. Syposium Ind. Electron. ISIE*, doi: https://doi.org/10.1109/ISIE.2017.8001446.

[17] J. Blanche, D. Flynn, H. Lewis, G. Couples, and R. Cheung, “Analysis of geomaterials using frequency-modulated continuous wave radar in the K-band,” in *First World Congress on Condition Monitoring*, 2017.

[18] J. Blanche *et al.*, “Analysis of Sandstone Pore Space Fluid Saturation and Mineralogy Variation via Application of Monostatic K-Band Frequency Modulated Continuous Wave Radar,” *IEEE Access*, vol. 6, pp. 44376–44389, 2018, doi: 10.1109/ACCESS.2018.2863024.

[19] J. Blanche, J. Buckman, H. Lewis, D. Flynn, and G. Couples, “Frequency Modulated Continuous Wave Analysis of Dynamic Load Deformation in Geomaterials,” in *Offshore Technology Conference*, 2020, doi: 10.4043/30479-ms.

[20] J. Blanche, “Frequency Modulated Continuous Wave Sensing for Static and Dynamic Material Analysis,” Heriot-Watt University, Edinburgh, 2020.

[21] J. Blanche *et al*., "Dynamic Fluid Ingress Detection in Geomaterials using K-Band Frequency Modulated Continuous Wave Radar," IEEE Access, vol. 8, pp. 111027 - 111041, 2020, doi: 10.1109/ACCESS.2020.3002147.

[22] O. Al-Khudairi and H. Ghasemnejad, “To improve failure resistance in joint design of composite wind turbine blade materials,” *Renew. Energy*, vol. 81, pp. 936–951, 2015, doi: 10.1016/j.renene.2015.04.015.

[23] B. H. Crespo, "Chapter 3: Damage Sensing in Blades," in *MARE-WINT: New Materials and Reliability in Offshore Wind Turbine Technology*, W. Ostachowicz, M. McGugan, J.-U. Schröder-Hinrichs, and M. Luczak Eds.: Springer, Cham, 2016, pp. 25-52. doi: 10.1007/978-3-319-39095-6_3

[24] K. Branner and A. Ghadirian, "Database about blade faults," DTU Wind Energy, 8793278098, 2014, vol. E. [Online]. Available: https://doi.org/10.13140/RG.2.2.14390.91207

[25] M. P. Y. Desmulliez, S. K. Pavuluri, and G. Goussettis, “Sensor System for Detection of Material Properties,” WO 2018/078401, 2018.